Nuclear Instruments and Methods in Physics Research A 751 (2014) 41–47

Contents lists available at ScienceDirect

Nuclear Instruments and Methods in Physics Research A

journal homepage: www.elsevier.com/locate/nima

# TCT measurements with slim edge strip detectors ☆

Igor Mandić [a,*], Vladimir Cindro [a], Andrej Gorišek [a], Gregor Kramberger [a], Marko Mikuž [a,b], Marko Zavrtanik [a], Vitaliy Fadeyev [c], Hartmut F.-W. Sadrozinski [c], Marc Christophersen [d], Bernard Phlips [d]

[a] Jožef Stefan Institute, Jamova 39,Ljubljana, Slovenia
[b] University of Ljubljana, Faculty of Mathematics and Physics, Jadranska 19, Ljubljana, Slovenia
[c] SCIPP, UC Santa Cruz, Santa Cruz, CA 95064, USA
[d] US Naval Research Laboratory, Code 7651, 4555 Overlook Ave., SW, Washington DC, 20375, USA

ARTICLE INFO

*Article history:*
Received 18 October 2013
Received in revised form
24 January 2014
Accepted 14 March 2014
Available online 21 March 2014

*Keywords:*
Micro-strip silicon detectors
Radiation hardness
Edge-TCT
Scribing
Cleaving
Passivation

ABSTRACT

Transient current technique (TCT) measurements with focused laser light on miniature silicon strip detectors ($n^+$-type strips on p-type bulk) with one inactive edge thinned to about 100 μm using the Scribe-Cleave-Passivate (SCP) method are presented. Pulses of focused IR ($\lambda = 1064$ nm) laser light were directed to the surface of the detector and charge collection properties near the slim edge were investigated. Measurements before and after irradiation with reactor neutrons up to 1 MeV equivalent fluence of $1.5 \times 10^{15}$ $n_{eq}/cm^2$ showed that SCP thinning of detector edge does not influence its charge collection properties.

TCT measurements were done also with focused red laser beam ($\lambda = 640$ nm) directed to the SCP processed side of the detector. The absorption length of red light in silicon is about 3 μm so with this measurement information about the electric field at the edge can be obtained. Observations of laser induced signals indicate that the electric field distribution along the depth of the detector at the detector edge is different than in the detector bulk: electric field is higher near the strip side and lower at the back side. This is a consequence of negative surface charge caused by passivation of the cleaved edge with $Al_2O_3$. The difference between bulk and edge electric field distributions gets smaller after irradiation.



## 1. Introduction

In standard silicon detectors, strips or pixels are surrounded first by several guard-rings followed by bulk material forming a clearance to the dicing line. This inactive part of the detector can be more than 1 mm wide. In such applications as medical imaging or high energy physics many detectors are tiled together to produce an extended sensitive area. Avoiding dead area in such systems is a non-trivial endeavor, and the inactive edges of detectors complicate the design of support structures, alignment etc. Reducing or even completely removing inactive detector edges is an important goal of detector development. There are several approaches to tackle this problem [1–5] and one of the techniques is the Scribe Cleave Passivate-SCP-method [6,7]. Standard dicing process leaves a detector edge with high density of defects and therefore low resistivity. Guard-rings are needed to prevent the electric field extending to the cut edge, which would usually result in high edge currents. With the SCP method the wafer surface is the first scribed by a laser or etching process and then the detector is cleaved along the scribed line oriented along a crystal plane. Cleaving leaves a surface with low defect density which is passivated in the next production step. In case of p-type material the edge is passivated with atomic layer deposition of $Al_2O_3$ [6,7]. This results in a highly resistive edge so that ideally guard rings are not needed any more. The SCP method is attractive because, unlike the active edge approach [3,5], it is a post processing method and can be used with any detector design, provided it is produced on a wafer with appropriate crystal orientation. It is also expected to be more cost effective because it does not require 3D or double-sided detector processing.

One of the important questions related to the slim edge detectors is the charge collection property of the area close to the detector edge because surface charge on the cleaved edge distorts the electric field. Measurements with SCP processed detectors before irradiation [1,8] showed that this is not a problem. In this paper we report on the measurements with silicon strip detectors

☆Work done in the framework of the CERN-RD50 collaboration.
* Corresponding author.
*E-mail address:* igor.mandic@ijs.si (I. Mandić).

http://dx.doi.org/10.1016/j.nima.2014.03.026
0168-9002/

with a single slim edge processed with the SCP method before and after irradiation with reactor neutrons.

Charge collection properties were examined with Transient Current Technique, TCT measurements. Pulses of IR ($\lambda = 1064$ nm) laser light, focused to a spot with a FWHM $< 8$ μm, were directed to the surface of the detector and detector's charge collection properties near the slim edge were investigated. IR light was used because of its long absorption depth ($> 1$ mm at $-20$ °C) in silicon. The laser pulse creates charge carriers throughout the entire detector thickness similar to the passage of an energetic charged particle.

Measurements were made also with focused red laser beam directed on the cleaved edge of the detector. Red light ($\lambda = 640$ nm) penetrates only $\sim 3$ μm into silicon and observation of electrical pulses induced by red laser light reveals information about the local electric field on the SCP processed detector edge.

## 2. Experimental setup

The setup – scheme can be seen in Fig. 1 – has already been described in several publications [9–12]. Short laser pulses (100 ps) were generated by equipment from Advanced Laser Diode Systems GmbH. Signals were amplified by a wide band amplifier (MITEQ AM-1309, 10 kHz–1 GHz) and digitized with a Lecroy 950 WavePro oscilloscope (1 GHz). The detector was connected to a high voltage power supply (Keithley 2410) through a Bias-T (Picosecond 5531, 750 kHz–10 GHz) to decouple the readout electronics from the high voltage applied to the strips. Laser light was focused to a spot with a FWHM $< 8$ μm. The detector was positioned in the laser beam with high precision translator stages (Newport M-ILS100PP) enabling two dimensional movements. The optical system was also mounted on a translator stage used for focus distance adjustment. The detector could be thermally stabilized in the range from $-20$ °C to 60 °C by a Peltier element. The measurements described here were all made at $T = -20$ °C. The equipment was flushed by dry air to prevent condensation and ice formation.

### 2.1. Detectors

Measurements were done with miniature ($\sim 1 \times 1$ cm$^2$) silicon strip detectors produced by CiS [13] as a part of ATLAS Planar Pixel Project submission [14]. The detectors are fabricated with n-type implants on 300 μm thick p-type Float Zone silicon with a resistivity such that the detector has a full depletion voltage $\sim 50$ V. The strip pitch is 80 μm. Implants are biased through polysilicon resistors from the bias ring and the metal readout strips are AC coupled. As mentioned above, one edge of the detector was thinned with the SCP method. Fig. 2 shows the photo of one detector and close-ups of the SCP edges of 4 detectors. The widths of SCP edges are different from device to device. The direction of the cut is not necessarily parallel to the direction of strips so the width of the edge written in the photo is only approximate at the shown detector side and the outer guard ring visible in the photo may not be complete. The detector named D0 has cut edge $\sim 220$ μm wide and 3 guard rings, D3 edge width $\sim 180$ μm and 1 guard ring, D4 width $\sim 110$ μm and no complete guard ring and D10 $\sim 180$ μm and 2 guard rings.

The bias voltage which could be applied before the onset of breakdown current varied between the detectors. Also the detector currents varied from detector to detector and were approximately a few μA at 20 °C up to a reverse bias voltage of 50 V before irradiation.

Each detector was connected to the high voltage power supply and to the readout amplifier with one bond wire connecting the bias ring and the line leading to the readout amplifier and Bias-T as shown in Fig. 3. Therefore, signals induced on the bias ring were observed. This was the simplest connection for measurements of signals induced as close as possible to the SCP processed edge allowed comparisons of signals induced near processed and standard detector edge as will be explained later. The detector back plane was in contact with a metal base plate kept at ground potential. The metal plate was thermally stabilized with a Peltier element.

Measurements were done before and after irradiation with reactor neutrons. Detectors were irradiated in the TRIGA reactor in Ljubljana [15] up to a 1 MeV neutron equivalent fluence $\Phi_{eq} = 1.5 \times 10^{15}$ n/cm$^2$. After irradiation detectors were annealed for 80 min at 60 °C.

### 2.2. Top-TCT measurements

In Top-TCT measurements an IR laser beam is directed onto the top surface of the detector, and the beam is scanned in 2.5 μm steps in the direction perpendicular to the strips as can be seen in

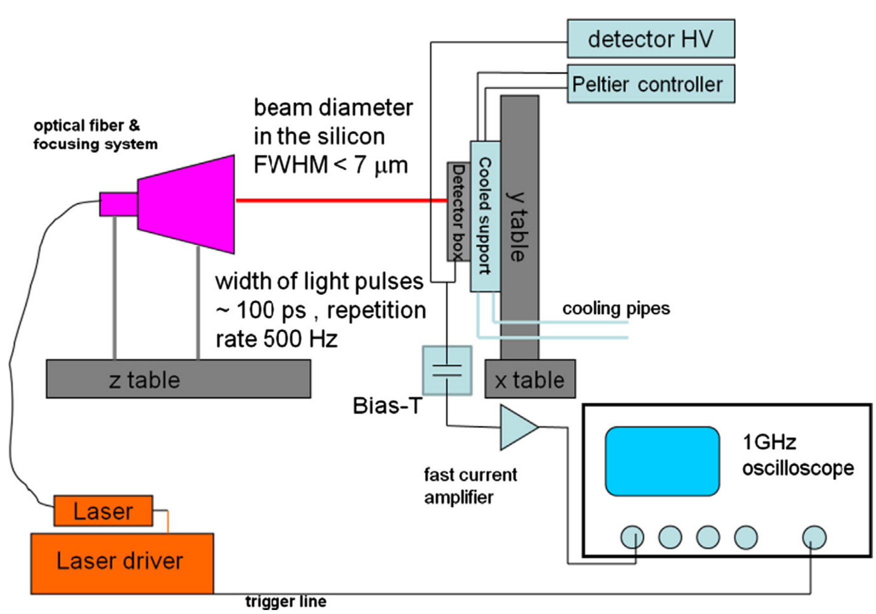


**Fig. 1.** Scheme of the experimental setup.

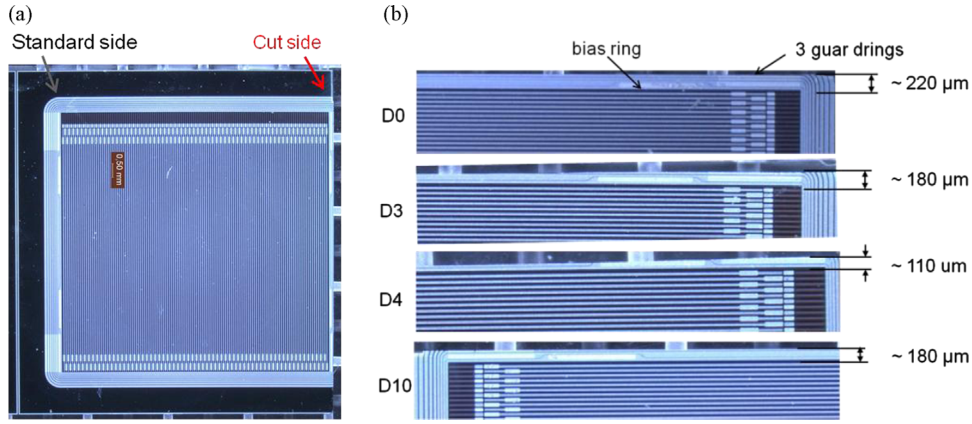


**Fig. 2.** (a) Photo of one detector with indicated standard and SCP edges, (b) close-ups of 4 detectors named D0, D3, D4 and D10 with SCP processed edge. The distance between SCP edge and the sensitive part of the detector is indicated in the figure. The photos were taken with detectors in a Gel-Pack.

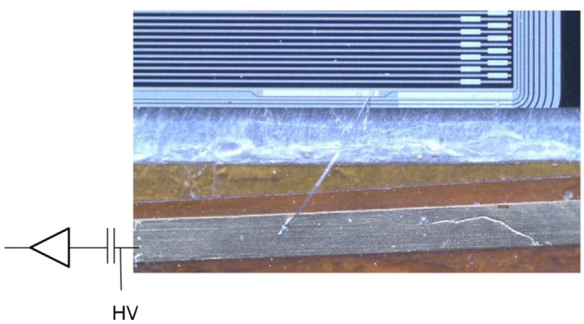


**Fig. 3.** The bond wire connecting the bias ring to the high voltage line can be seen. The same line was connected also to the readout amplifier via a Bias-T.

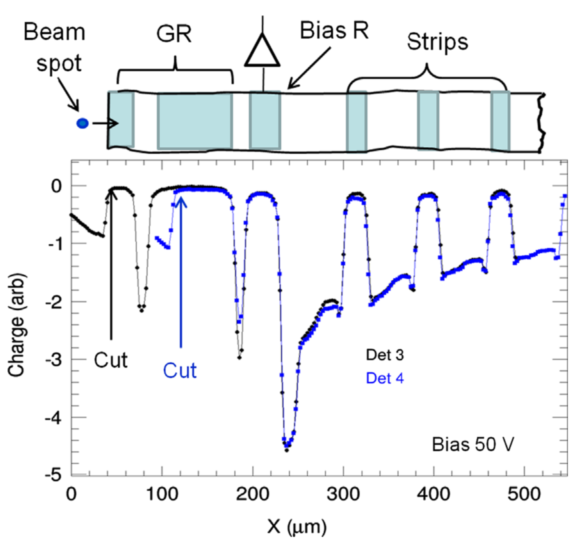


**Fig. 4.** Charge collection profile measured with Top-TCT with IR laser. The scheme above the graph explains the connections and the arrow indicates the direction of laser beam scan. Metalized regions are shown in blue color. Each point represents the charge measured at this location of the beam. Measurements with detectors D3 and D4 are shown in the same figure, normalized to the same charge at one measurement point, at $x = 500\ \mu$m. The positions of the SCP cuts are indicated in the figure. They are different for the two detectors. (For interpretation of the references to color in this figure legend, the reader is referred to the web version of this article.)

Fig. 4. At each beam position 400 pulses were averaged. Time integral of the pulse from 0 (the time of the laser pulse production) to 25 ns was calculated offline. The pulse is proportional to the current induced by the moving charge in the detector therefore the time integral of the pulse is proportional to the collected charge.

A measurement of collected charge from a scan of the IR laser beam across the surface of the detector is shown in Fig. 4, together with the drawing explaining the measurements. As can be seen, zero (or very small, because of laser beam tails) charge is measured when the laser beam is directed on the metal surfaces. The charge measured left of the cut is due to light entering the detector through the side surface because of reflections from the mounting plate, because of conical shape of the beam with focus plane on the detector surface and also because of imperfect alignment. Collected charge falls as the beam moves away from the bias ring because of the shape of weighting field (Ramo's field) [16]. Only the bias ring has low impedance connection with the amplifier so this field (which describes capacitive coupling), gets smaller with increased distance. Implants are biased from bias ring over large resistors ($>1\ \mathrm{M\Omega}$) and the electric field shape is as in normally connected strip detector. Therefore the carriers released by the laser pulse drift along field lines at the nearest strip but the charge collected in 25 ns on the bias ring falls with the distance because of smaller capacitive coupling.

The graph in Fig. 4 shows measurements with two detectors with different widths of the SCP processed edge. Measured charge values from a scan over one detector were scaled with a single factor so that they agree at one measured value with another detector. This was done to allow a comparison between the results, since the charge scale depends on mounting, focus and laser power, which is in general not reproducible between the samples. It can be seen in Fig. 4 that measured charge in the sensitive part of the detector, i.e. on the strip side of the bias ring, does not depend on the width of SCP edge. This result is in agreement with measurements described in Refs. [1,8] where it was shown that charge collection efficiency of detector is not affected by the proximity of SCP edge.

Similar scan as described above can be done also across the standard, not SCP cut edge (see Fig. 2) of the detector. In Fig. 5 comparison of charge measured in a scan across the standard and cut edge is shown. Coordinates of standard side scan are transformed (by a mirror image and shift) so that the two measurements can be shown in the same plot. No significant difference between charges induced by laser light in the sensitive part of detector on cut or standard side at the same distance from the bias ring was observed in measurements shown in Fig. 5. Measurements shown in Fig. 5 were made at the largest bias voltages, which could be applied before the onset of breakdown current. At these bias voltages, the non-irradiated detector, Fig. 5a, and detector D4 irradiated to $\Phi_{eq} = 1\times10^{14}\ \mathrm{n/cm^2}$ (bias = 250 V), in

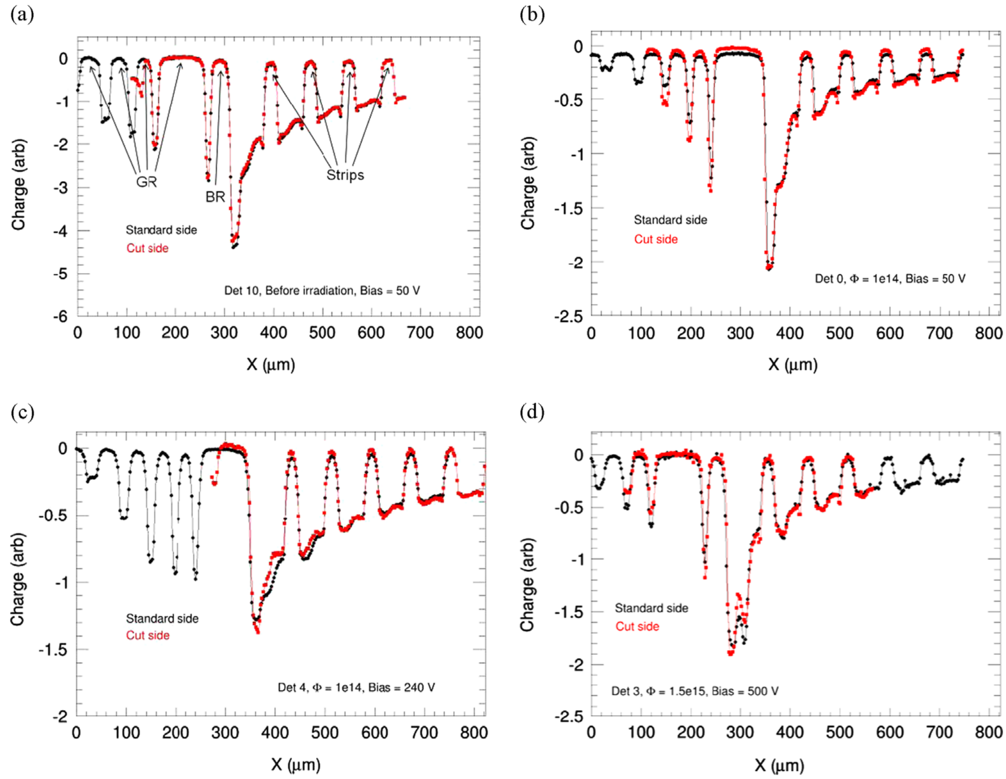


**Fig. 5.** Comparison of charge measured in IR laser scan across the standard and cut side of the detector. Figure (a) shows measurements with detector D10 before irradiation. Guard rings (GR), bias ring (BR) and strips are indicated in the figure. Other figures show similar situation: strips are on the right of the peak with most negative charge while bias ring followed by the guard rings are on the left. Figure (b) shows detector D0 irradiated to $\Phi_{eq}=10^{14}$ n/cm$^2$ and biased with 50 V, (c) detector D4, $\Phi_{eq}=1\times10^{14}$ n/cm$^2$, biased with 240 V and (d) detector D3, $\Phi_{eq}=1.5\times10^{15}$ n/cm$^2$, Bias = 500 V.

Fig. 5c, were fully depleted while bias voltages in measurements in Fig. 5b and d were below full depletion.

Measurements shown in Fig. 5a confirm results shown in Fig. 4 and further prove that charge collection is not affected by the SCP processed edge in not irradiated detectors. But it is important to note that measurements if Fig. 5 were made also with irradiated detectors. Therefore these results strongly indicate that charge collection near the SCP processed edge does not behave differently from the standard edge after neutron irradiation. But it should be mentioned that measurements should be repeated with detectors irradiated with charged particles because total ionizing dose (TID) effects on the properties of the cut edge surface cannot be excluded at this point.

### 2.3. Edge-TCT measurements

Edge-TCT measurements were made with red laser light ($\lambda=640$ nm). Red light was chosen because it penetrates only $\sim 3\ \mu$m into silicon and the induced current is sensitive to the electric field at the SCP processed detector edge. The scheme in Fig. 6 explains the measurement setup. Scans of detector edge with focused red laser light had been used previously [17] to study edgeless detectors.

Pulses measured at different depths (coordinate $y$ on scheme in Fig. 6) and bias voltages are shown in Fig. 7. Note that the polarity of pulses was changed to positive offline. It can be seen that the initial slope (at $t\sim0$) of the pulse is less steep as the distance increases. According to Ramo's theorem [16] induced current is proportional to the product of weighting field and carrier velocity and therefore to the electric field. Weighting field for the connection shown in Fig. 6 falls with coordinate $y$ (see Fig. 6) but the change is not very rapid at the detector edge. There are large gradients of Ramo's field in very close vicinity of the bias ring electrode while at the SCP edge, which is more than 100 µm away, the variations are smaller. For example, absolute value of weighting field 30 µm into the detector from the SCP edge (to take into account that carriers would not drift on the surface but would spread into the detector) falls by a factor of 3 from $y=0$ µm to $y=300$ µm. In Fig. 7(a) pulses at $y\geq150$ µm are initially very low because carriers are created in the region with very low electric field. The change of the initial slope of the signal from $y=10$ µm to $y=150$ µm is much larger than factor of 3 so it cannot be caused by the change of weighting field alone. The induced current qrises after the carriers reach higher electric field region by slow drift or diffusion. As expected, at higher bias voltage (150 V in Fig. 7(b) steeper initial slopes are observed at larger

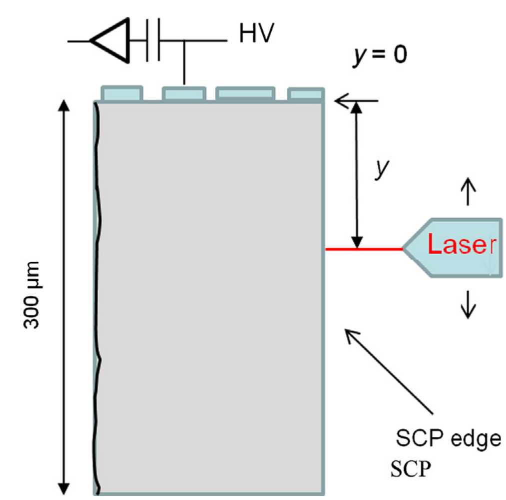


**Fig. 6.** Scheme explaining the Edge-TCT measurement.

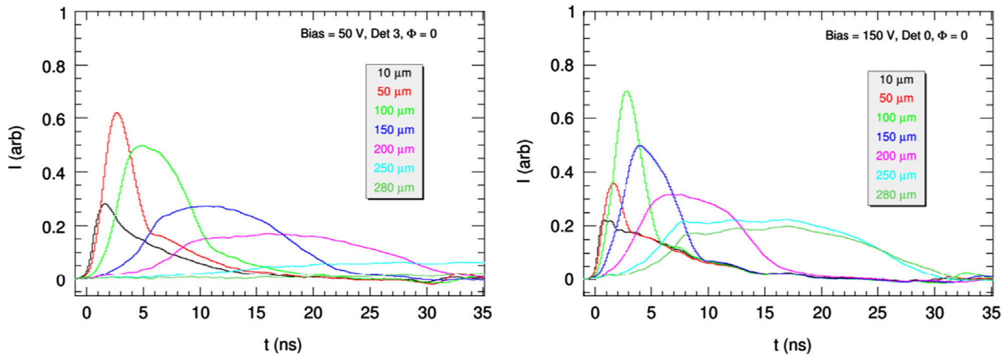


**Fig. 7.** Edge-TCT pulses measured at different distances of laser beam from the top (coordinate $y$ in Fig. 6) at different bias voltages. Polarity of pulses was changed to positive offline.

depths than at lower bias in Fig. 7(a). However, signals at $y \geq 250$ μm are still very low at the beginning indicating that the electric field is weak at this depth even at 150 V. One should keep in mind that full depletion voltage of these detectors before irradiation is ~50 V. These measurements therefore show that electric field profile close to the detector edge is different than away from it in the detector bulk.

The field dependence on depth can be better seen in Fig. 8 where the induced current measured 600 ps after the laser pulse is plotted as a function of laser position. According to the "prompt current method" [10,18], which follows from the Ramo's theorem [16], immediately after the short laser pulse, before the carriers could move significantly, the induced current can be written as

$$I(y, t \sim 0) \approx qE_w[\overline{v}_e(y) + \overline{v}_h(y)] \tag{1}$$

$$\overline{v}_e(y) + \overline{v}_h(y) \propto E \tag{2}$$

where $q$ is the charge, $E_w$ is the weighting field and $v_e$ and $v_h$ are average carrier velocities. If electric field is not too high (up to few V/μm at room temperature) carrier velocities are proportional to the electric field (Eq. (2)). As was already mentioned, the weighting field $E_w$ is not constant so the pulse height profile is not directly proportional to the electric field profile. But weighing field change is much smaller than the signal changes shown in Fig. 8 which strongly indicates that the electric field at the edge is very weak for $y > 200$ μm even at Bias = 150 V which is well over the depletion voltage. These conclusions are in agreement with the observations from Fig. 7.

Such electric field distribution is expected because of the surface charge on the SCP processed edge [7,19], which is a consequence of passivation of the cut edge with $Al_2O_3$. Fig. 9 shows results of calculation of the potential at the corner of the strip detector with and without surface charge on the detector edge. In the modeled detector, bulk was p-type silicon with space charge concentration $7.5 \times 10^{11}\ q_0/\mathrm{cm}^3$, $q_0$ is elementary charge, full depletion voltage $V_{fd} = 50$ V. Strips, bias ring and guard ring, which in this model extends to the edge of the detector, were $n^+$ implants with concentration $10^{20}\ q_0/\mathrm{cm}^3$. Equipotential lines were calculated by numerically solving the Poisson equation (more detailed in [20]) in two dimensions. As can be seen in Fig. 9, negative surface charge on the cut edge causes concentration of equipotential lines near the detector corner resulting in a small potential drop on the large part of the edge even if bias voltage is above the full depletion voltage. In the case of no surface charge (Fig. 9a) the potential distribution at the edge is similar to that in the detector bulk and electric field is present through the whole detector depth.

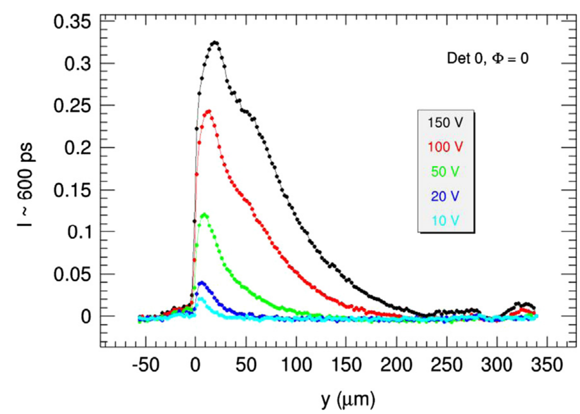


**Fig. 8.** Induced current measured 600 ps after the laser pulse as a function of distance from the strip plane (coordinate $y$) at different bias voltages.

### 2.4. Edge-TCT with irradiated detectors

The distribution of initial induced pulse amplitude measured over the SCP edge at different bias voltages from the detector irradiated to $\Phi_{eq} = 1.5 \times 10^{15}$ n/cm$^2$ is shown in Fig. 10. It can be seen that electric field is larger at the strip side than at the back side of the detector similar as for the not irradiated detector shown in Fig. 8. (note that absolute values of $I(\sim 600$ ps) cannot be compared between different detectors, only the curve shapes).

However, measurements shown in Fig. 10 were done at bias voltages below the full depletion voltage which is about 1.8 kV after irradiation with $\Phi_{eq} = 1.5 \times 10^{15}$ n/cm$^2$. The depth to which the detector is depleted can be roughly estimated from the relation for planar geometry

$$w = \sqrt{\frac{2\varepsilon\varepsilon_0 V}{q_0(N_{eff0} + g_c \Phi_{eq})}} \tag{3}$$

where $w$ is the depleted depth, $N_{eff0} = 7.4 \times 10^{11}$ cm$^{-3}$ is the effective space charge before irradiation corresponding to $V_{fd} =$ 50 V, $g_c = 0.017$ cm$^{-1}$ is the introduction rate for stable damage for p-type float zone material irradiated with neutrons from [21] and $\Phi_{eq}$ is 1 MeV equivalent neutron fluence. The constants $\varepsilon$, $\varepsilon_0$, $q_0$ are relative silicon permittivity, vacuum permittivity and elementary charge, respectively.

The value calculated with Eq. (3) can be compared with the value of coordinate $y$ on Fig. 8 or Fig. 10 at which falling edge $I$ ($t \sim 600$ ps) gets low – below 3 times the value of the spread of baseline fluctuation. This can be interpreted as the coordinate $y$ at which the electric field gets low. The comparison of measured coordinate $y$ and calculated depths is shown in Fig. 11 for detectors

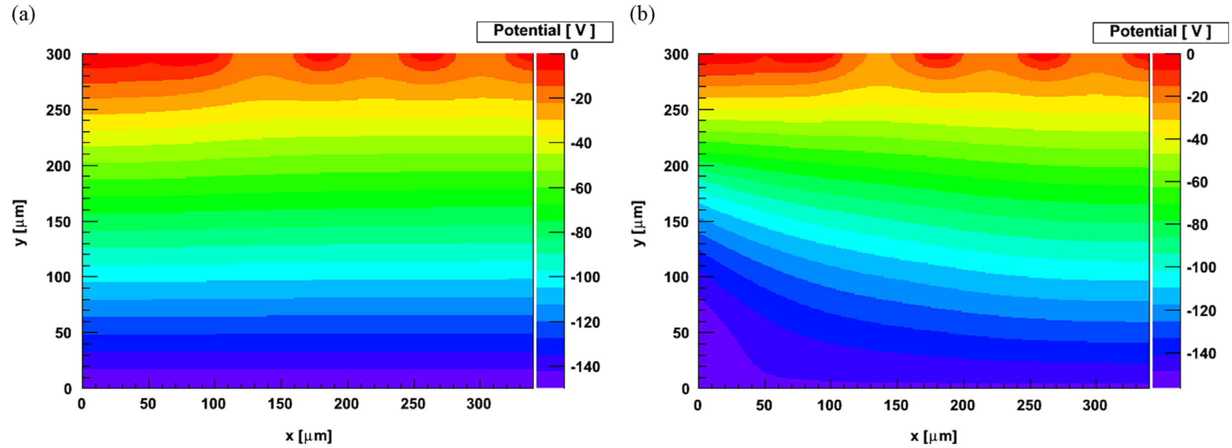


**Fig. 9.** Calculation of the potential in cross section near the corner of a strip detector. The strip side is on the top, cut edge on the left. Figure (a) shows the situation with no surface charge and figure (b) with negative surface charge of $-3\times10^{10}\ q_0/\mathrm{cm}^2$, where $q_0$ is elementary charge. The calculation was done for Bias = 150 V on detector with full depletion voltage $V_{fd}=50$ V. Note that in this model coordinate $y=0$ is on the back side of the detector while in measurements $y=0$ is at the strip side.

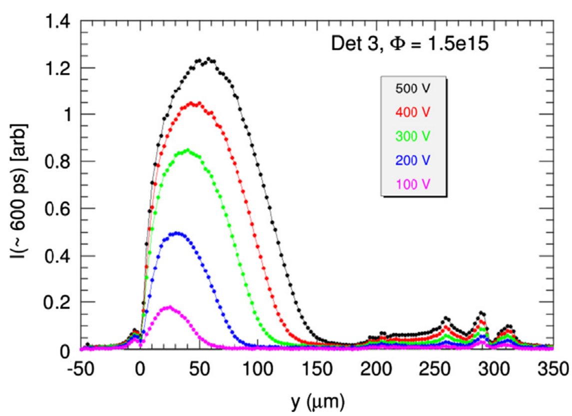


**Fig. 10.** Induced current amplitude measured 600 ps after the laser pulse as a function of distance from the strip plane at different bias voltages for detector irradiated to $\Phi_{eq}=1.5\times10^{15}$ n/cm$^2$.

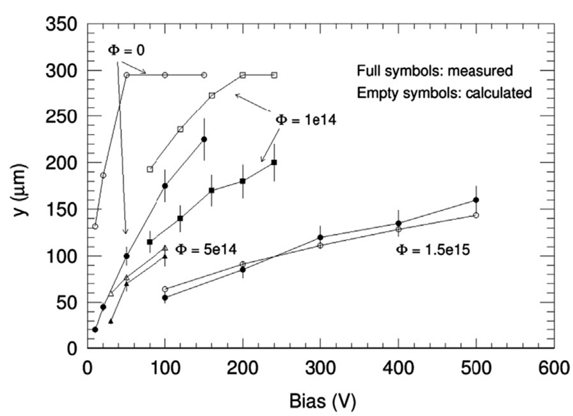


**Fig. 11.** Comparison of calculated depletion depth and the depth at which initial induced current $I(t\sim600$ ps) on the detector edge measured with red light laser gets low.

irradiated to different fluences. It can be seen in Fig. 11 that the difference between calculated depletion depth using Eq. (3), in which no surface charge is considered, and measured coordinate at which $I(t\sim600$ ps) gets low, is large for $\Phi_{eq}=0$ and $\Phi_{eq}=10^{14}$ n/cm$^2$. This indicates that for these two cases the influence of surface charge is important and it bends the equipotential lines and so increases electric field closer to the strip side as can be seen also in Fig. 9b. At higher fluences the difference between measured and calculated values in Fig. 11 is small. This indicates that the influence of surface charge on electric field is small in comparison with the space charge caused by neutron irradiation so the electric field at the detector edge is not significantly different from the field in the detector bulk (see Fig. 9a).

## 3. Conclusions

In this work TCT measurements with silicon strip detectors with one slim edge processed with the SCP method are presented. Measurements were made with detectors with slim edge widths – distances from the edge to the sensitive part of detector – in the range between 100 and 250 µm. Two types of measurements were performed: measurements with focused infrared laser with long penetration depth directed to the surface of the detector to measure charge collection properties near the processed edge and measurements with focused red light (penetration depth ~3 µm) directed at the detector edge to probe electric field on the surface of the SCP treated detector edge.

It was shown that the proximity of SCP edge does not influence charge collection properties in un-irradiated detectors and in detectors irradiated with reactor neutrons up to $\Phi_{eq}=1.5\times10^{15}$ n/cm$^2$. This is a promising result for further development of SCP technique for detector edge slimming.

Measurements with red laser confirmed the prediction that the accumulation of negative surface charge on the SCP processed edge due to passivation with $Al_2O_3$ would cause squeezing of equipotential lines to the top (strip) side of the detector. The consequence is a distorted electric field profile with low electric field close to the back side of the detector even at relatively high bias voltages. Measurements with IR light indicate that this field distortion does not extend far from the edge because charge collection in the sensitive part of detector ~100 µm away is not affected by the edge. The results with irradiated detectors indicate that the difference between the electric field profile at the edge and in the detector bulk gets smaller with increasing neutron fluence.


## Acknowledgments

The authors would like to thank the crew at the TRIGA reactor in Ljubljana for help with irradiation of detectors. The research leading to these results has received funding from the European Commission under the FP7 Research Infrastructures project AIDA, grant agreement no. 262025. We would like to thank the Institute for Nanoscience (NSI) at the U.S. Naval Research Laboratory (NRL) and the NSI staff. The work done at NRL was sponsored by the Office of Naval Research (ONR).The work at SCIPP was supported by U.S. Department of Energy, grant DE-FG02-04ER41286.

## References

[1] R. Bates et al., Characterisation of edgeless technologies for pixelated and strip silicon detectors with a micro-focused x-ray beam, 2013, JINST 8 P01018.
[2] TOTEM collaboration, E. Noschis, et al., Nuclear Instruments and Methods A 563 (2006) 41.
[3] C. Kenney, J. Segal, E. Westbrook, S. Parker, J. Hasi, et al., Nuclear Instruments and Methods A 565 (2006) 272.
[4] S. Eränen, et al., Nuclear Instruments and Methods A 607 (2009) 85.
[5] S. Altenheiner, C. Gossling, J. Jentzsch, R. Klingenberg, T. Lapsien, et al., Planar slim-edge pixel sensors for the ATLAS upgrades, 2012 JINST 7 C02051.
[6] V. Fadeyev, et al., Nuclear Instruments and Methods A731 (2013) 260.
[7] M. Christophersen, V Fadeyev, B.F Phlips, H.F.-W. Sadrozinski, C Parker, S Ely, J.G Wright, Nuclear Instruments and Methods A 699 (2013) 14.
[8] R. Mori et. al, Charge collection measurements on slim-edge microstrip detectors, 2012 JINST 7 P05002.
[9] M. Zavrtanik et al., Position sensitive TCT evaluation of irradiated 3D-stc detectors, 2007 IEEE NSS Conference Record, pp. 1318–1321.
[10] G. Kramberger, V. Cindro, I. Mandić, M. Mikuž, M. Milovanović, M. Zavrtanik, K. Žagar, IEEE Transactions on Nuclear Science NS-57 (2010) 2294.
[11] M. Milovanović et al., Effects of accelerated long term annealing in highly irradiated $n^+$-p strip detector examined by Edge-TCT, 2012 JINST 7 P06007.
[12] I. Mandić et al., TCT measurements of irradiated strip detectors with a focused laser beam, 2013 JINST 8 P04016.
[13] CiS Forschungsinstitut fur Mikrosensorik und Photovoltaik GmbH, ⟨http://www.cismst.org⟩.
[14] M. Beimforde, Nuclear Instruments and Methods A 636 (2011) S8.
[15] L. Snoj, G. Žerovnik, A. Trkov, Applied Radiation and Isotopes 70 (2012) 483.
[16] S. Ramo, Currents induced by electron motion, in: Proceedings of the IRE, 1939, vol. 27, p. 584.
[17] E. Verbitskaya, et al., Nuclear Instruments and Methods A 604 (2009) 246.
[18] G. Kramberger et al., Electric field modeling in heavily irradiated silicon detectors based on Edge-TCT measurements, PoS – Proceedings of Science, Vertex 2013, 022.
[19] M. Christophersen et al., Laser-scribing and $Al_2O_3$ sidewall passivation of p-type sensors, 6th Trento Workshop on Advanced Silicon Radiation Detectors (3D and P-type Technologies), Trento, Italy, 2 March 2011. ⟨http://tredi.fbk.eu/⟩.
[20] G. Kramberger, V. Cindro, M. Mikuž, Nuclear Instruments and Method A 457 (2001) 550.
[21] V. Cindro, et al., Nuclear Instruments and Method A 599 (2009) 60.